Biomass and Bioenergy 142 (2020) 105800

Contents lists available at ScienceDirect

Biomass and Bioenergy

journal homepage: http://www.elsevier.com/locate/biombioe

Synthesis of porous activated carbon powder formation from fruit peel and cow dung waste for modified electrode fabrication and application

Rajabathar Jothi Ramalingam [a,*], M. Sivachidambaram [b,d], J. Judith Vijaya [b,**], Hamad A. Al-Lohedan [a], M.R. Muthumareeswaran [c]

[a] Surfactant Research Chair, Chemistry Department, College of Science, King Saud University, Riyadh, 11451, Saudi Arabia
[b] Catalysis and Nanomaterials Research Laboratory, Department of Chemistry, Loyola College (Autonomous), Chennai, 600 034, India
[c] King Abdullah Institute for Nanotechnology, College of Science, King Saud University, Riyadh, 11451, Saudi Arabia
[d] Department of Chemistry, Theivanai Ammal College for Women, Villupuram- 605602, Tamilnadu, India

ARTICLE INFO

Keywords:
Porous carbon
Calcination
Phosphoric acid
Solid waste
A. heterophyllus
Cow dung
Activated carbon

ABSTRACT

Porous activated carbon (PAC) powder is prepared from solid bio-wastes such as jack fruit peel waste (AP) and cow dung samples (CD). The activation process is carried out by phosphoric acid treatment followed by calcination at different temperature condition. XRD pattern confirms the amorphous phase formation with graphitic nature for different precursor utilization. BET Surface area measurement are showing higher surface area values for both AP and CD precursor route derived carbon samples. FE-SEM analysis shows the uniform and hierarchical porous network formation and aggregated particle with tiny nanotube and spherical carbon nanoparticle morphology obtained in TEM analysis. X-ray analysis confirms the formation of graphitic carbon and porous morphology for sample activated at increased calcination temperature. TEM images of JF carbon samples are shows spherical nanoball and nanotube morphology. The elemental composition of as prepared carbon samples is determined by SEM-EDX and confirms the formation major carbon content existence. The electrochemical property is analyzed by various electrochemical tools and it shows stable activity for super capacitor application. Nickel foil based modified electrode was fabricated using as prepared activated porous carbon material. The Cs (specific capacitance) of the carbon sample activated at high temperature (900 °C) shows 324 and 347 F/g AP-9 and CD-9 samples. The comparative surface property characterization and detailed electrochemical property was carried out between peel waste and cow dung derived porous activated carbon samples through cyclic voltammetry, Galvano static charge-discharge and electrochemical impedance spectroscopy analysis.

1. Introduction

The solid waste management and renewable energy demands are important field of research to adoption of low cost methodology for solid waste utilization [1–4]. Preparation of porous activated carbon (PAC) materials with micro and mesoporosity could be very useful in the field of green chemistry catalysis and renewable energy applications [5–8]. The micro and mesoporous nature of carbon materials are strongly depending on the usage of raw material and preparation methodology including the mass ratio between bio char or pre carbonized carbon (PCC) and activating agent followed by calcination temperature condition. The above points are also important for efficient electrode materials fabrication for EDLC (electrochemical double layer capacitance) [9–11]. Yuan et al. recently fabricated carbon powder from plastic waste and it is also a global environmental pollution treatment problem [12,13]. Waste polymer plastic bottles were carbonized and activated using KOH or NaOH to develop porous carbons materials and they studied the activity of prepared carbon materials for CO_2 storage applications [12]. The potential use of agricultural waste sources with additional treatment for the removal of anionic pollutants such as chlorides, fluorides etc., from water was examined [14–16]. In another related study, ultrasonic method is adopted to prepare the porous carbon materials derived from agricultural waste and tested their activity for electro chemical super capacitor application [17,18]. Treatment by ultrasonic irritation causes deeply etch carbon material to develop more porous structure to the resulted porous carbon network. The presence of additional pore

* Corresponding author.
** Corresponding author.
E-mail addresses: jrajabathar@ksu.edu.sa (R. Jothi Ramalingam), jjvijaya78@gmail.com, judithvijaya@loyolacollege.edu (J.J. Vijaya).

https://doi.org/10.1016/j.biombioe.2020.105800
Received 3 May 2020; Received in revised form 20 September 2020; Accepted 27 September 2020
Available online 5 October 2020
0961-9534/

Scheme 1. Two stage preparation strategy of phosphoric acid activated PCC from Cow dung and Jackfruit peel waste (AP).

structures is beneficial for the transfer of electrolytes, providing more active sites and improving electrochemical performance. Compared with the samples prepared without ultrasonic treatment ultrasonic treatment enhances the activity [18–21]. The activated carbon by ultrasonic route prepared modified electrodes exhibits a high specific surface area of 1281 m_2/g, abundant porous structure and prominent specific capacitance of 197 F/g. Bio char is widely recognized as a multifunctional material, developing high-performance carbon materials from bio char for both energy and environmental applications remains challenging [22–25]. Torreya grandis seeds inner-shell, a widespread lignocellulose biomass waste was used to synthesize hierarchically porous carbon materials via a different carbonization/activation approach [26]. The prepared bio char exhibited excellent energy storage performance in sodium sulphite (1 M Na_2SO_4) with a large capacitance, high-rate capability, and favorable stability (97% capacitance retention after 5000 cycles). Recently great efforts have been focused on converting bio-waste into high-valued carbon material. However, it is still a great challenge to achieve high carbon yield and controllable porous size distribution for researchers. Hence, porous carbon synthesized from using multi-void structure of waste coffee ground beans into hierarchical porous carbon was reported and thy adopted the combination of catalytic carbonization and alkali activation methods [27]. Agricultural waste derived banana peel activated carbon (BPAC)) as a sustainable and easily available biomass resource and recently sulphur-doped banana peel-derived activated carbon based modified electrode was successfully tested for super capacitor application [28]. The results of modified electrode show that the formation of improved high surface area of 2224.9 m^2/g, a large pore volume of 0.77 cm^3/g, and a suitable pore-size distribution of approximately 0.8 nm for Sulphur doped bana peel derived carbon materials. It is easy to bring Sulphur-doped banana peel produced carbon (S-BPAC) into contact with an electrolyte and it shows the specific capacitance of 162.5 F/g [28].

Jackfruit is commonly used in South part of India and adopted in most of the southeast Asian cuisines. *Artocarpus heterophyllus* (*A. heterophyllus*) is a botanical name for Jackfruit. India is the origin of specific type of oval shaped Jackfruit (*A. heterophyllus*-**AP)** and it is extended up to tropic regions [29,30]. For *A. heterophyllus(AP)*, is not seasonal fruit and it is harvested throughout the year [30]. *A. heterophyllus* have a seed, fruit and peel in outside portion. The outside portion of the peel is thrown away as a waste material, and it results in the high output of *A. heterophyllus* peel (AP). AP have no commercial value and in fact it often creates a serious problem in solid waste disposal. In the present study, Conversion of peels of AP and cow dung (CD) waste into carbon powder would increase its economic value, help to reduce the cost of waste disposal, and provide an inexpensive raw material for fabrication of effective modified carbon based electrodes. Instead of conventional way of activation by alkali, in the present study phosphoric acid is utilized to activate the PCC (pre carbonized carbon) into porous activated carbon such as AP-PAC (activated carbon derived from peel waste) and CD-PAC (activated carbon from cow dung waste). The highlight of the work is to adopted Clay molded Graphite Crucible (CMGC) is low cost reactor to create vacuum for calcination process carried out at different temperature condition. The as prepared carbon sample have been characterized for structural, morphological, porous nature and electrochemical performance. The comparative electrochemical performance of as prepared porous carbon samples are demonstrated using modified nickel foil electrode setup for super capacitor applications.

2. Experimental

2.1. Preparation of AP and CD type porous activated carbon samples

Jackfruit peel waste and dry cow dung waste are used as the starting material to prepare pre carbonized carbon (PCC). The raw materials are collected from villages in Villupuram district, Tamil Nadu, India. First step is to cut the peels into small parts like 5 cm square shapes and dried cow dung sample was crushed in the powder form. After dried at room temperature, the peels are washed with distilled water several time, followed by dried for one day at 80 °C in the case of cow dung sample washing is not required. The dried peel waste and cow dung samples was transferred in a graphite crucible separately. The as prepared filled

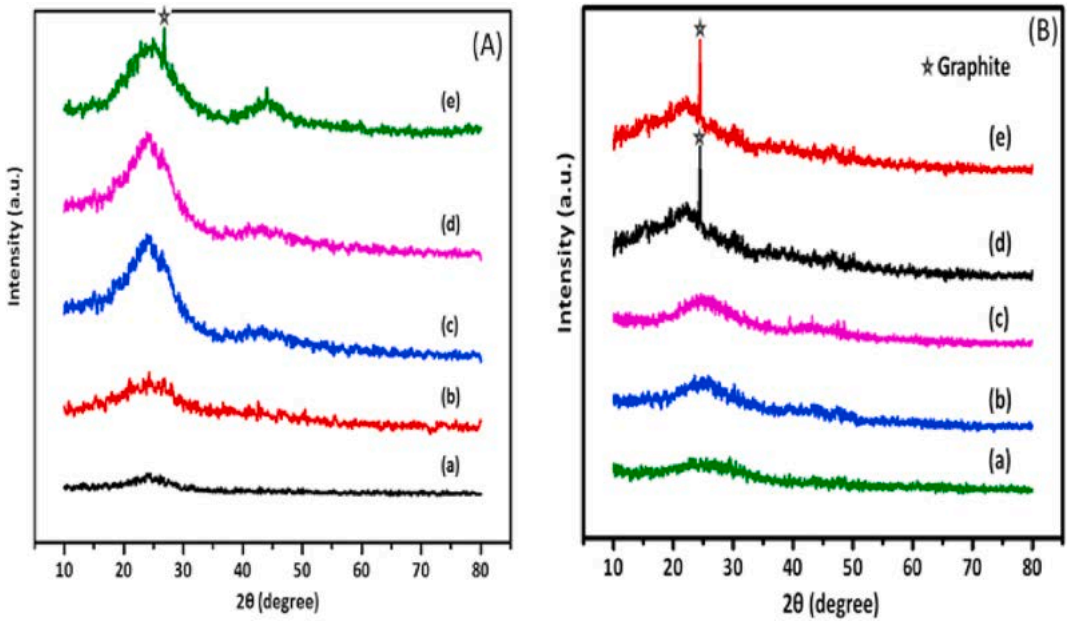

Fig. 1. X-ray diffraction patterns of (A) (a) AP-PCC, (b) AP 6, (c) AP 7, (d) AP 8 and (e) AP 9.

crucible is further sealed by a clay molding method. The molding is done by simply heating the crucible with help sandy clay available in the earth crust, after pasted with clay followed by tightly closed the mouth of the crucible. The autogenic vacuum created inside the crucible and minimal amount of oxygen present inside the closed crucible. The clay molded graphite crucible was placed in a muffle furnace at 400 °C for 4 h under autogenic vacuum conditions. Finally, the above prepared PCC sample was collected from the graphite crucible by breaking the molded clay using the hammer followed by grinding the sample in mortar and pistol. The minimum amount of silica present in the clay exist with activated carbon sample. The as prepared graphite mixed activated carbon is obtained in the form fine carbon powder.

Second step is the preparation of activated carbon by phosphoric acid activation method, 20 g of fine carbon prepared from peels waste and cow dung prepared by above method (PCC) was mixed with the activating agent (H_3PO_4) in the ratio of 1:4 (1 wt percentage of PCC and 4 wt % of equivalent phosphoric acid) and fine carbon powder and phosphoric acid stirred for 3 h at 80 °C. After stirring, the sample was filtered and dried at 80 °C for 24 h. Finally, the as prepared phosphoric acid activated PCC is further calcined at different high temperate (600, 700, 800 and 900 °C) for 4 h under vacuum conditions and the respective sample designated as AP-600, AP-700, AP-800 and AP-900. Again, the clay molded graphite crucible was utilized to avoid oxygen atmosphere in the heat treatment process. The above calcined carbon samples are washed 3 to 4 time using distilled water to maintain a neutral pH followed by dried at 80 °C for one day. Scheme 1 demonstrates the schematic diagram of the preparation stages of porous activated carbon. The as prepared samples are designated as AP-6, AP-7, AP-8, AP-9 for peel waste derived carbon sample and cow dung derived carbon samples designated as CD-6, CD-7, CD-8 and CD-9.

2.2. Characterization

All chemicals are used in the present study purchased from Sigma Aldrich and utilized without further purification. The crystalline phase characterization of as prepared porous carbon samples were characterized by X-ray diffraction spectra (XRD). Bruker D8 advance X-ray diffractometer with Cu Kα source was adopted to analyze the samples. Fourier transform infra-red (Ft-IR) analysis was performed to identify the presence of surface functional group present in the as prepared carbon samples (Shimadzu FTIR-8400S spectrophotometer). Brunauer-Emmett-Teller (BET) surface area and pore size measurement was analyzed by Micromeritics ASAP 2020. The morphology and microstructures of the porous carbon was studied by a scanning electron microscope (JSM 6490-LV from JEOL), and a high-resolution transmission electron microscopy (FEI Tecnai G20). Particle size and zeta potential measurement were recorded using Nano plus particle analyzer.

2.3. Electrode fabrication and electrochemical measurements

The activated carbon based modified 50 mm thickness nickel foil electrode was prepared by using 16 mg of as-prepared porous carbon (AP or CD) with 2 mg of poly (vinylidene difluoride) binder followed by mixing acetylene black (2 mg). To the above mixture few drops of n-methyl pyrrolidinone is added as an organic solvent to made a paste. Then the paste was coated in a nickel foil (1 × 1 cm) and it serves as a working electrode. The cyclic voltammetry (CV), Galvano static charge-discharge (GCD), electrochemical impedance spectroscopy (EIS) studies are carried out to explore the Supercapacitors applications using Ametek PARSTAT 4000 instrument. Silver chloride electrode and platinum wire is used as reference and counter electrode, respectively. The following equation are utilized to calculate the super capacitance values of the respective carbon modified electrode in various electrochemical analysis (eqs. (1) and (2)). Cs is specific capacitance and I is the current density (A/g), Δ*t* - charge-discharge time (seconds), m is the mass (g) and Δ*V* is the working potential window of the electrode (V/s).

$$C_s = \int \frac{\Delta I}{2\ Vm(v_2 - v_1)}\, dV \text{ i.e.} \Delta I = I_a - I_c \quad (1)$$

$$Cs = I \times \Delta t/m \times \Delta V \quad (2)$$

3. Results and discussions

3.1. Crystalline structure and function group characterization

X-ray diffraction study reveals the crystalline or amorphous properties of the as prepared porous carbon derived from AP and CD. The XRD patterns of AP-PAC samples are shown in Fig. 1a. The porous carbon prepared from different raw materials (peel waste and cow dung) are showing amorphous nature for all calcined samples (Fig. 1a and b).

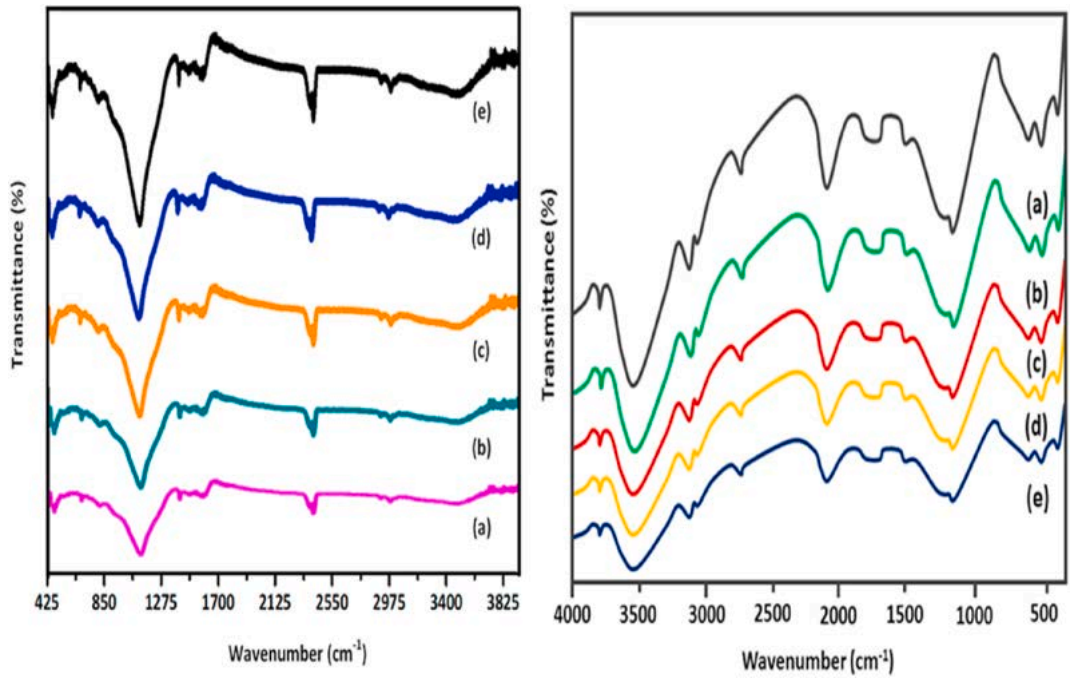

Fig. 2. Ft-IR spectra of (A) (a) AP-PCC, (b) AP 6, (c) AP 7, (d) AP 8 (e)AP-9; (B) (a) PCC (b) CD-1 (c) CD-2 (d) CD-3 (e) CD-4.

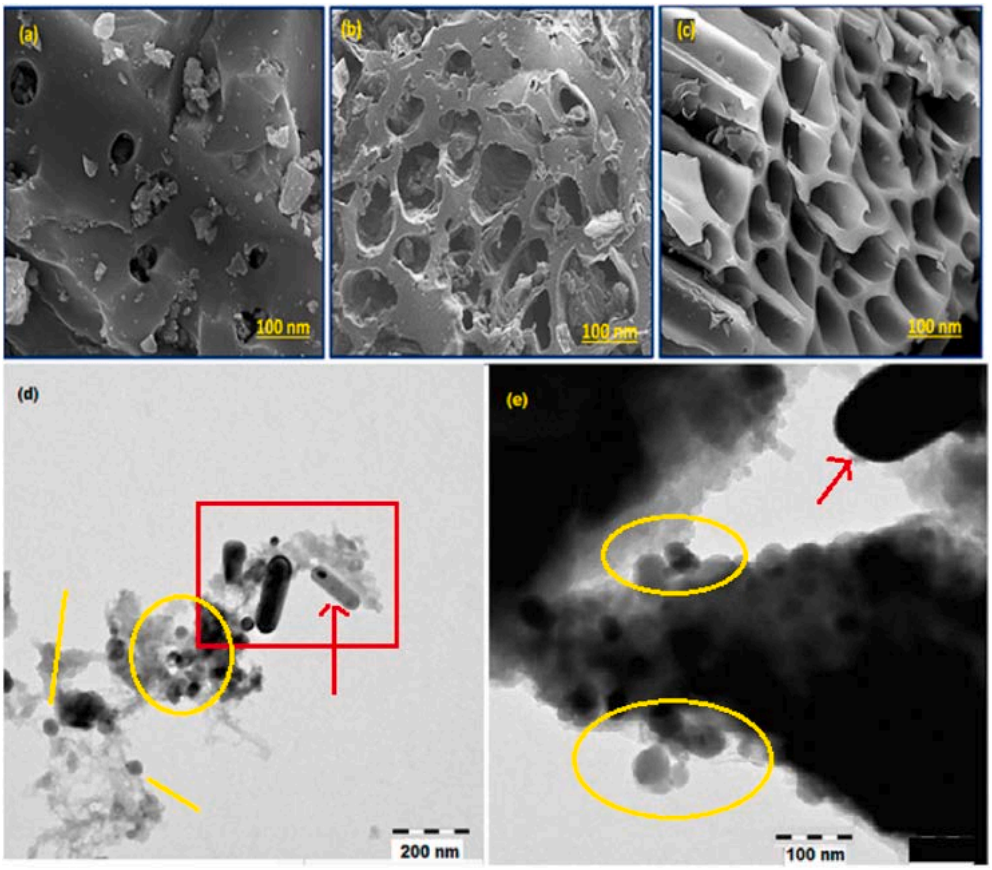

Fig. 3. Scanning electron micrographs of (a) AP-6 (b) AP-8 (c)AP-9; Transmission electron micrographs of (d–e) AP-9.

The two 2θ peaks for both precursor route prepared sample are identified at 23° (100 plane) and around 43° (101 plane), are similar to other alkali method prepared activated carbon samples [JCPDS number 75–2078]. The JCPDS data of activated carbon matches very well with our XRD results [31,32]. The peak at 26° (002 plane) due to presence of the graphitic carbon, which is from the calcination process of carbon sample carried out in graphite crucible causes the sharp graphitic peak.

Ft-IR spectra is useful to understand the nature of functional group or

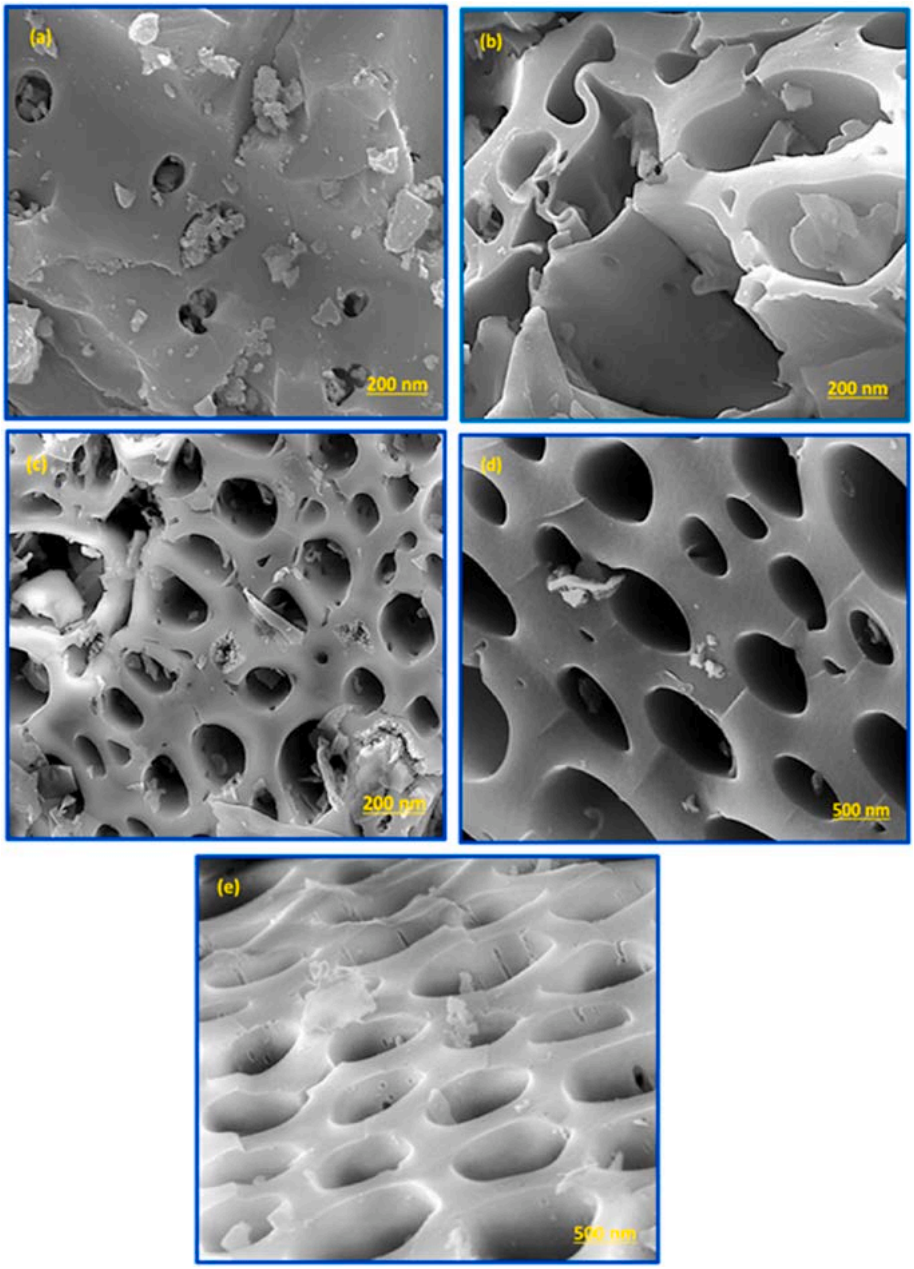

Fig. 4. Scanning electron micrographs of (a) CD-PCC, (b) CD 6, (c) CD 7, (d) CD 8 and (e) CD 9 PAC samples.

surface bound species present in the AP and CD derived porous carbon samples such as AP 6, AP 7, AP 8 and AP 9 and the same was shown in Fig. 2a. In Fig. 2a, from PCC to AP-9 shows the similar functional group frequency and it further confirms that the phosphoric acid activated carbon formation. The shoulder peak at 1090 cm^{-1} was due to presence of phosphorous oxygen linkage exist in the surface of carbon network and ionized phosphate esters. The absorption at 1381 cm^{-1} due to presence of carbon-oxygen bonds of alcohol, esters, and carboxylic acid groups. The peak at 3435 cm^{-1} and 750 cm^{-1} indicates the presence of Oxygen-Hydroxyl hydrogen, carboxylic acidic group and Silicon-hydroxyl bonds present on the as prepared carbon samples are originated from the clay molded crucible sources. An aromatic Carbon-=Carbon stretching was observed at 1566 cm^{-1} and the presence of hydrocarbon chains shown the absorption peak at 1455 cm^{-1}. Similar trend and functional group frequency are observed in the case of cow dung sample (Fig. 2b), only peak intensity difference occurred for CD-6, CD-7, CD-8, CD-9 samples. The should peak and peak associated with phosphorus group are not existed in the alkali method prepared activated carbon samples, which is confirmed from the reported Ft-Ir studies [33,34]. Existence of phosphate and phosphine and silicon bonds could improve the surface activity of the porous carbon samples for catalytic and electro catalytic reactions.

3.2. Morphological studies

High resolution SEM micrographs of AP-porous carbon samples are shown in Fig. 3a-c. Fig. 3a exhibited the morphology of the as-prepared pre carbonized carbon (PCC) it shows rough and not uniform porous morphology. Fig. 3b and c shows the SEM images of AP-7 and AP-9. The number of pores on the surface of the AP derived carbon sample (AP-9) is much more than AP-7 as shown in Fig. 3. The creation of new pores is caused by the activating agent (H_3PO_4) at increased temperature condition above 800 °C and it burns the carbon to form more uniform pores. Similarly, AP-7 has exhibited a smoother surface and less degree of

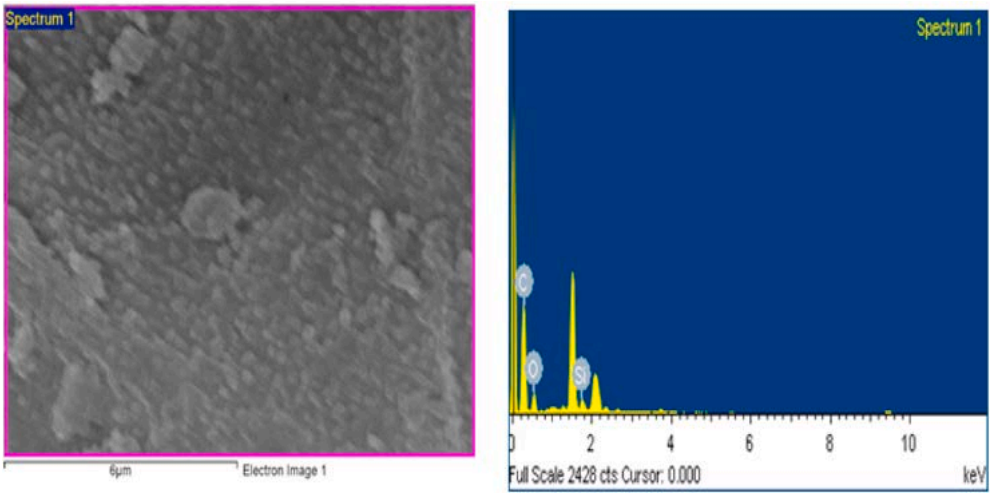

Fig. 5. SEM-EDX spectra of peel waste derived activated porous carbon calcined at 700 °C (AP-7).

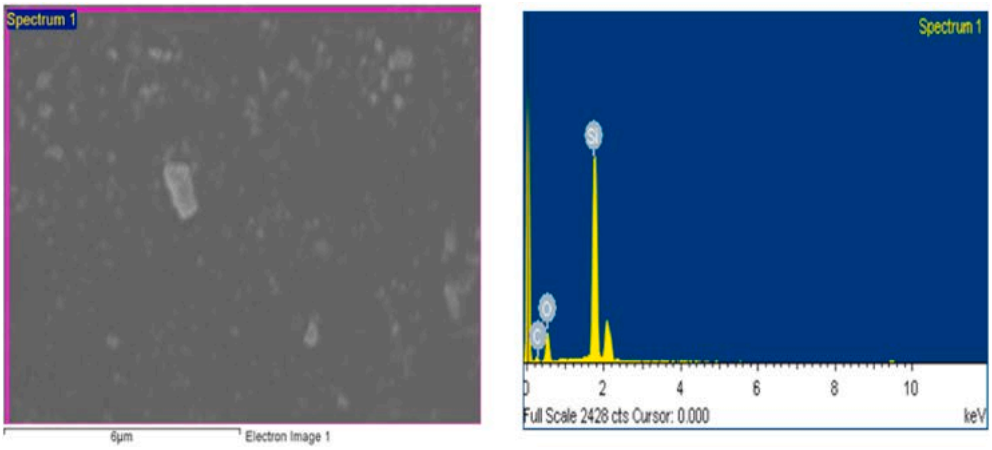

Fig. 6. SEM-EDX spectra of peel waste derived activated porous carbon calcined at 900 °C (AP-9).

porosity, when compared to AP 9. The uniform porous morphology improvements between the AP samples (AP 6, AP 7, AP 8 to AP 9). The H_3PO_4 usage for activation process and calcination of clay molding at high temperature condition caused multi architecture with interior-exterior porous surface for the prepared carbon samples.

Furthermore, the morphological and structural studies of the AP-9 sample was done by the high resolution TEM (HR-TEM) which showed the spongy glassy like morphology with metallic rich carbon particles formation with graphitic layers as shown in Fig. 3d and e. The graphitic nature of carbon samples was further deeply magnified below 100 nm scale and it depicted that the agglomerated spherical nanoball (red circled in Fig. 3d) and tiny carbon nanotube (yellow square marked in Fig. 3e) formation occurred as shown in Fig. 3d. This type of inter-connected spherical nanoball shaped porous activated carbon particles (Fig. 3e) would provide a unique open pore system with high active surface area and a short diffusion path for electrolyte ions.

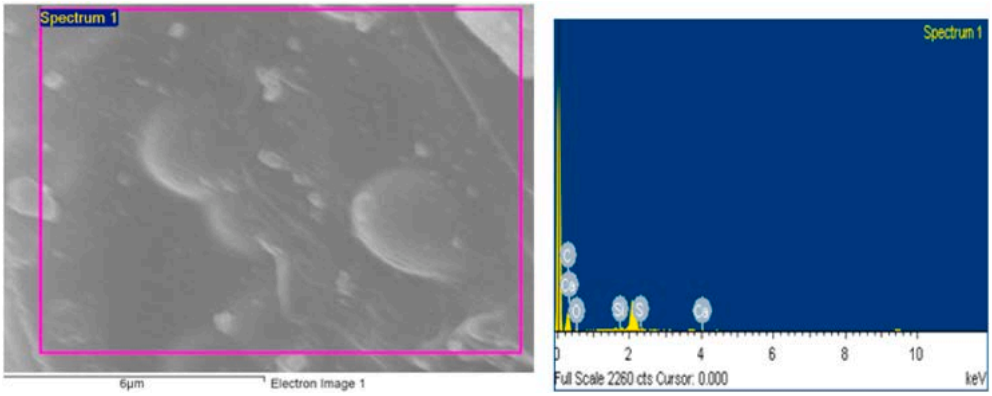

Fig. 7. SEM-EDX spectra of cow dung derived activated porous carbon calcined at 900 °C (CD-9).

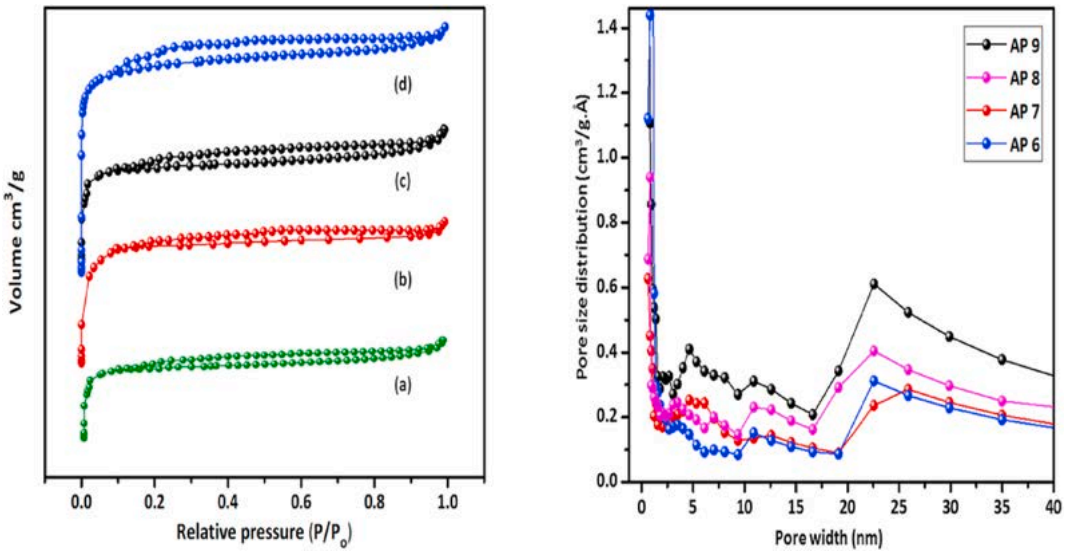

Fig. 8. Nitrogen adsorption-desorption analysis and Pore size distribution analysis of (a) AP-6 (b) AP 7, (c) AP 8 (d)AP-9.

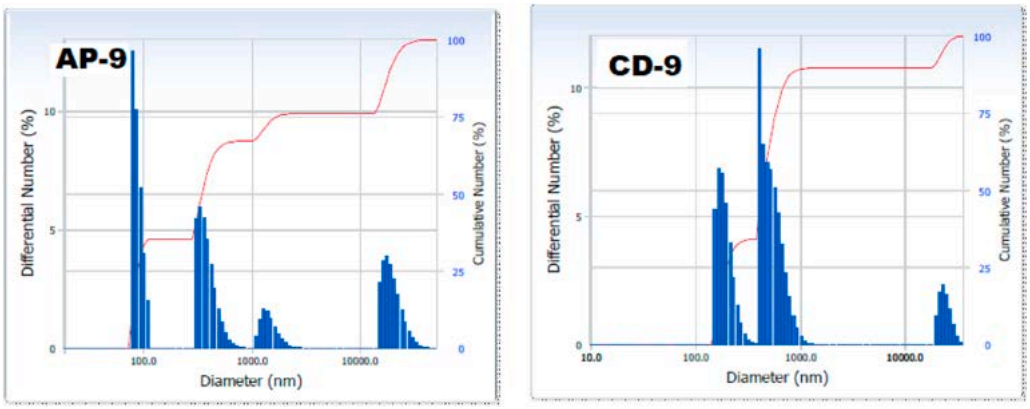

Fig. 9a. (a) Particle size analysis peel waste derived AP-9 and cow dung derived CD-9.

Fig. 4a-e shows the as-prepared CD-PCC had rough surface and the absence of porosity. The number of pores on the surface of the CD porous activated carbon sample CD 6 to CD 9 is much more than for CD 6 and is shown in Fig. 4a-c. The number of pores seem to be increased with increasing the activation temperature in the activation processes. The creation of new pores is caused by the activating agent (H_3PO_4) and it burns the carbon to form the pores. Similarly, CD 6 has exhibited a smoother surface and less degree of porosity, when compared to CD 9, which shows the presence of hierarchical pore structure and irregular pores (Fig. 4e). Also, the CD 9 sample exhibits the arrangement of pore channels that are interconnected with each pore channels and it is a promising one for EDLC.

The elemental composition of peel waste and dried cow dung derived porous activated carbon was analyzed by SEM-EDX techniques. Figs. 5–7 shows the presence of carbon, oxygen and silicon content as prepared AP-7 and AP-9 and CD-9 samples. The carbon sample heat treated at high temperature has also showing silicon content and silicon element arising from the clay molding preparation in graphite crucible [35]. Porous activated carbon and contains 74.5 at% of carbon and 24.5 at% of oxygen and less than 1 at% of silicon (AP-9) and in the case of AP-9 shows the little higher percentage for silicon (1.73 at %), carbon (76.6 at%), oxygen (22%). In the case of cow dung sample (CD-9), in addition to silicon content Sulphur content also exist in final form of porous activated carbon. Fig. 7 shows the EDX spectra of cow dung derived carbon sample exist with major carbon content of 84 at%, oxygen content exist as 11.79 at%, Si (0.97 at%) and Sulphur (1.94). Other impure element present in the activated carbon due to nature of starting materials and clay molding graphite crucible utilization in the preparation process of porous activated carbon [36,37]. Fig. 9(a and b) shows the Particle size and Zeta potential measurement of selected peel waste and cow dung derived carbon sample was carried out by Nano plus analyzer using laser light scattering method. Fig. 9a shows the Number distribution of carbon particle size obtained in aqueous medium. The different particle size distribution was occurred in the as prepared AP-9 and CD-9 sample. AP-9 carbon sample was shown average particle size formation close to 100 nm and in the case of CD-9 carbon sample shows the higher than 100 nm particle size and it extends up to 1000 nm. It is clear that the formation of smaller carbon particle depends on starting material usage. Fig. 9b shows the negative zeta potential values for both AP-7 and AP-9 sample and less zeta negative potential means increase in their conductivity property. The conductivity of as prepared carbon sample increase by increasing activation temperature. AP-9 has higher conducting capacity than all other AP-PAC samples.

3.3. Surface area, textural and adsorption–desorption characterization

Pore structure and BET surface area of as prepared carbon samples from peel waste are evaluated by N_2 adsorption-desorption isotherms. Fig. 8 shows adsorption-desorption isotherms at 77 K for four AP-PAC

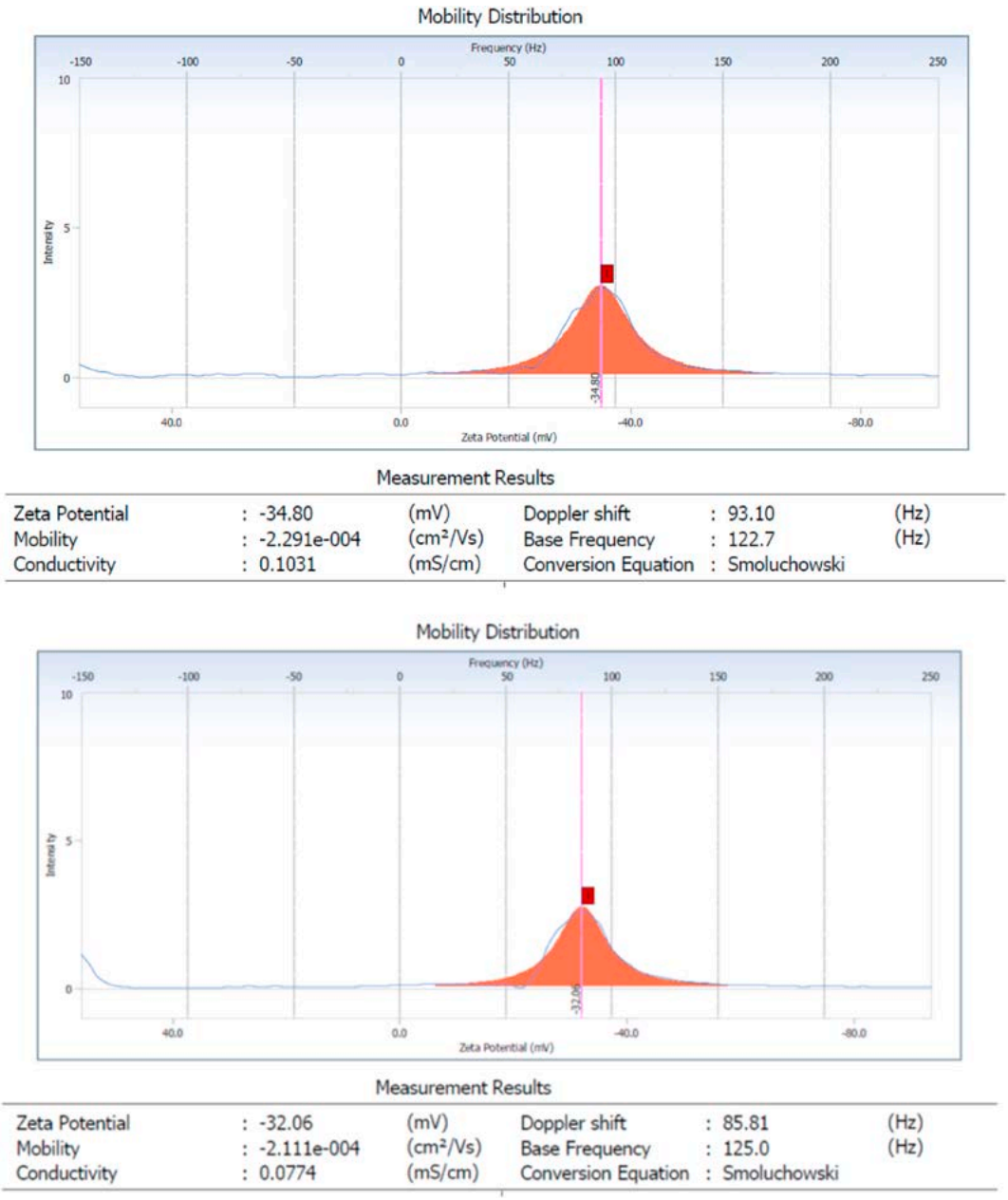

Fig. 9b. (b) (i) Zeta potential measurement of activated porous carbon calcined at 700 °C (AP-7) (ii) Zeta potential measurement of activated porous carbon calcined at 900 °C (AP-9).

Table 1
Sample code, surface area, pore volume and average pore diameter of AP derived PAC samples.

Samples	S_{BET} (m^2/g)	S_{micro} (m^2/g)	S_{meso} (m^2/g)	V_{Total} (cm^3/g)	V_{micro} (cm^3/g)	V_{meso} (cm^3/g)	D_p nm
AP 6	689	492	197	0.495	0.301	0.194	2
AP 7	984	637	347	0.664	0.435	0.229	4
AP 8	1260	823	437	0.869	0.571	0.298	8
AP 9	1585	993	592	0.965	0.635	0.330	10

[a] BET surface area,[b] Micropore surface area, [c] Mesopore surface area,[d] Total pore volume, [e] Micropore volume, [f] Mesopore volume, [g] Average pore diameter.

samples (AP-6, AP- 7, AP- 8 and AP- 9) with respective surface area values such as AP-6 = 689 m^2/g, AP- 7 = 984 m^2/g, AP- 8 = 1260 m^2/g and AP- 9 = 1585 m^2/g (Table 1) and surface area value of CD-9 (carbon derived from cow dung) showing highest surface area value of 2450 m^2/g, respectively [38]. Based on IUPAC classification of Hysteresis loop H4 type adsorption desorption occurred due to some pore blocking and ink-bottles porous nature for the present method prepared carbon samples. Pore size distribution analysis shows (Fig. 8) that the existence of micro (less than 2 nm) and mesoporous existence (pore size peak exists between 2 nm and 20 nm) for the prepared carbon samples. The porous carbon heated (calcination) at high temperature indicates that the, AP 9 has high micro and mesoporous (0.635 and 0.330 cm^3/g) than all other carbon sample (AP-6, AP-7 and AP 8). With an increase in activation temperature, the micropores are widened to the maximum and it is converted to mesoporous [39].

Role of phosphoric acid is playing crucial role in improves the porous structure with micro and mesoporous by intercalation of phosphate species in to the internal network of carbon chains at high temperature calcination process [40,41]. Due to calcination process at increased temperature causes gradual increase in surface area values and pore size

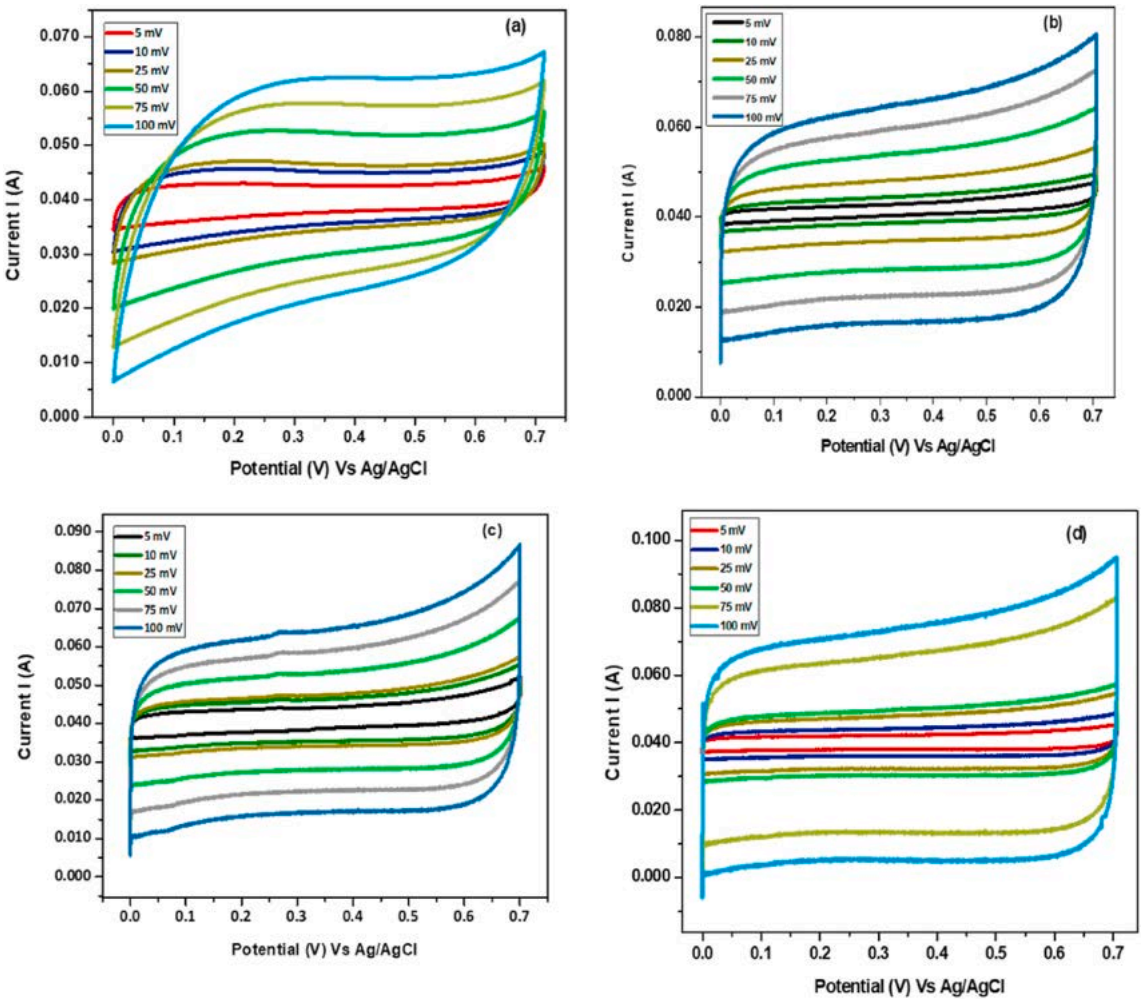

Fig. 10. Cyclic voltammograms of (a) AP 6, (b) AP 7 (c) AP 8 and (d) AP 9 samples.

Table 2
Specific capacitance from cyclic voltammetry (CV), galvanostatic charge-discharge (GCD) and electrochemical impedance spectroscopy (EIS) of AP-PAC sample.

AP-PAC Samples	Specific capacitance of CV (F/g)	Specific capacitance of GCD (F/g)	Double layer capacitance of EIS (F/g)
AP 6	168	165	162
AP 7	205	203	204
AP 8	268	284	272
AP 9	324	320	320

distribution from AP-6 to AP-9 samples.

4. Electrochemical characterization of peel waste and cow dung derived carbon based nickel foil electrodes

4.1. Cyclic voltammetry studies

Cyclic voltammetry analysis is shown in Fig. 10. The CV profiles of AP 6 and AP 7 show a low and imperfect rectangular image (Fig. 10 (a, b)), thus indicating that the less super-capacitive property. Ideal electrochemical active electrode material are generally shows large rectangular cyclic voltammetry curves [42]. N_2 adsorption-desorption analysis of AP 8 and AP 9 sample depicts improved surface area with hierarchical porosity. High pore size distribution and surface area are playing important role in the creation of the strong double layer formation at electrode surface. Fig. 10(c and d) shows CV curves for AP8 and AP-9. The exact symmetrical box-like shape for CV curves obtained for AP-9 and CD-9 (not shown) carbon sample due to good porosity and improved surface area.

The calculated specific capacitance is given in Table 2 and its displayed at different san rates (5 mV/s to 100 mV/s), when the scan rate increases, C_s values are decreases for all the prepared carbon samples. At low scan rate of 5 mV/s, theAP-9 sample implies a good charge propagation, quick ion diffusion within the pores and fast re-organizing of the electrical double layer at different potentials. The results indicated that the increase in temperature increased the porosity rapidly from AP 6 sample to AP 9.

4.2. Galvanostatic charge–discharge studies

Galvanotactic charge-discharge (GCD) studies is another route to study the electrochemical properties of the AP-PAC samples at various current density [43]. Fig. 11a-d show GCD waves of AP carbon sample prepared at different temperature treatment (AP 6, AP 7, AP 8 and AP 9). The studies carried out at various fixed current densities of 1A/g, 3 A/g and 5 A/g values and altering the potential (V) with respect to time (sec) plot showing the triangular shaped curve. In the case of AP 6 exhibits slanting portion in the triangle shape at low current density, slight IR drop occurred and also shows the low internal resistance. The other carbon samples like AP 7 and AP 8 sample has very slight slanting portion and it indicates the small internal resistance. In the case of AP 9

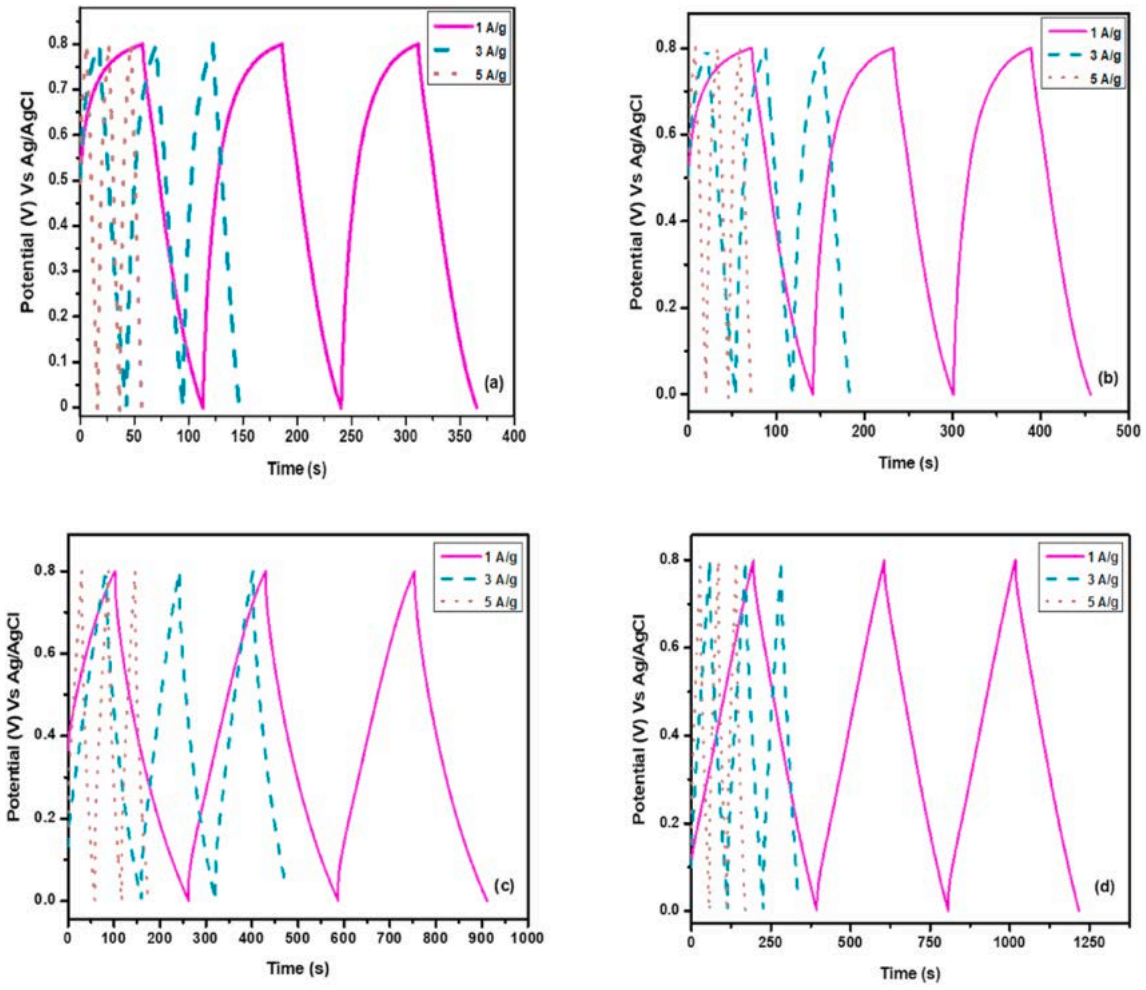

Fig. 11. Galvanostatic charge-discharge profiles of (a) AP 6, (b) AP 7, (c) AP 8 and (d) AP 9 PAC samples.

Table 3
Specific capacitance from cyclic voltammetry (CV), galvanostatic charge-discharge (GCD) and electrochemical impedance spectroscopy (EIS) of CD-PAC samples.

CD-PAC Samples	Specific capacitance of CV (F/g)	Specific capacitance of GCD (F/g)	Double layer capacitance of EIS (F/g)
CD 6	148	146	142
CD 7	215	213	207
CD 8	294	291	286
CD 9	347	347	338

sample shows the perfect linear lines with obvious sharp triangular shapes at low and high current densities. This reveals that the AP 9 electrode sample has very good capacitive behavior, when compared with other AP carbon samples. From equation (2), specific capacitance values are calculated using GCD results [32,44,45].

Table 2 show respective specific capacitance values derived by GCD analysis and it also compared with Cs values obtained from Cyclic Voltammetry studies. Due to stronger interaction at double layer interface between the electrode and electrolytes cause the higher capacitance value for AP- 9 and it results attains the higher charge-discharge time intervals at low current density values. In the case of electrochemical performance of cow dung derived carbon samples are also showing equivalent and much higher Cs values for sample CD-9. Table 3 shows the capacitance values calculated from Cyclic voltammetry (CV), GCD and impedance studies were used to explore the efficiency of the as prepared cow dung route prepared PAC samples (CD 6, CD 7, CD 8 and CD 9) are shown in Fig. 12. Cyclic voltammograms of cow dung derived carbon are also shows similar leaf like shape for CD 6 sample and CD 7 sample. CD 8 and CD 9 sample reveals more or less perfect rectangular shape. Sample CD 9 has obtained the ideal behavior properties of electric double layer capacitors. The specific capacitance (C_s) was calculated from the below formula. Hence, from the result of electrochemical analysis, CD 9 sample shows high specific capacitance with high BET surface area than CD 6, CD 7 and CD 8 samples due to role of activation temperature in the calcination process. At higher temperature conditions causes the development of new pores and channel arrangement (see Table 1).

4.3. Electrochemical impedance spectroscopy

The Nyquist plot and electrochemical impedance analysis of peel waste and cow dung derived carbon modified electrode was carried out at the frequency range of 0.1–100 kHz at OCP (open circuit potential) maintained at 5 mV. Fig. 12, shows the comparative electrochemical impedance measurement and the inset figure shows the fitted equivalent circuit of the respective samples.

All the impedance measurements were carried out in three electrode system using 1 M Na_2SO_4 as the electrolyte, the usage of neutral electrolyte to prevent and avoid corrosion in the Nickel foil electrode and also it acts as toxic free electrolyte. From Fig. 12, AP-6 to AP-9 samples shows slight broader in Nyquist plot compared to more narrow curves obtained in the case of cow dung derived carbon samples. Impedance

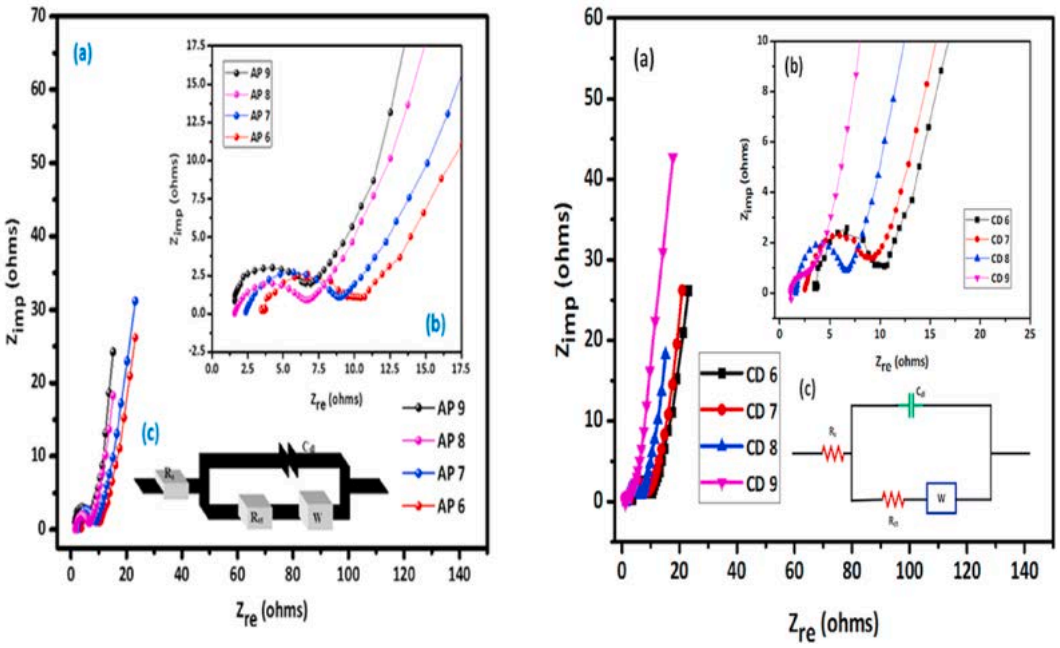

Fig. 12. Nyquist plot for porous activated carbon AP and CD samples (peel waste and cow dung derived) using a sinusoidal signal of 5 mV over the frequency range of 100 kHz to 1 mHz. Z_{re} is real impedance and Z_{imp} is imaginary impedance.

Table 4
Parameters for AP-PAC samples obtained from electrochemical impedance spectroscopy measurements.

Sample	R_s (Ω)	R_{ct} (Ω)	ESR (Ω)	W (Ω)
AP 6	0.72	5.48	5.20	0.845
AP 7	0.53	2.79	2.21	0.423
AP 8	0.34	1.56	1.40	0.140
AP 9	0.18	0.84	0.86	0.016
CD-8	0.57	3.17	2.19	0.305
CD-9	0.35	1.13	1.37	0.033

analysis is showing clear evidence for the difference of activated carbon modified electrode fabricated from two difference bio-waste source.

The fitted equivalent circuit consists of following parameters such as R_s, R_{ct} and W. R_s represents the solution resistance or intrinsic resistance, R_{ct} = charge transfer resistance, W is the Warburg resistance [46]. The equivalent circuit denotes the both capacitance system and resistivity in the system. In the case of porous materials deposited electrodes, Nyqusit plot can be separated into three parts: high frequency region, medium frequency region, low frequency region. In the high-frequency region, the Nyquist plot is semicircle and the real axis intercept is the equivalent series resistance and it is equal to the difference between the solution resistance (R_s) and charge-transfer resistance (R_{ct}) of the Nyquist plot. Table 4 shows the calculated parameters derived from electrochemical impedance analysis. Rs is keep on decreases from AP-6 to AP-9 and it represent the increased conductivity obtained for AP-9. The width of the semicircle impedance loop related with charge transfer resistance in the electrode materials. As shown in Fig. 12, the width is of semicircle is higher in the case of AP carbon samples compared CD samples. Rs and Rct values of CD samples area much lower than AP carbon sample. The second intersection points of the semicircles and the horizontal axis show the inner resistances (ESR) and it also shows the same trend for AP and CD sample. The ESR value of AP-9 sample (0.86) compared CD-9 sample (1.37). Inner resistance is higher in the case of CD derived carbon sample [47]. The more vertical line shows the more ideal capacitive behavior. The inset graph of Fig. 9 shows that there is an apparent semicircle in the high-frequency range in the EIS spectrogram of AP 9 and CD 9 modified electrodes. The electric double-layer capacitance respective to the charge transfer resistance. Table 5 shows the comparative physico chemical property and capacitance efficiency of reported and our method prepared porous activated carbon derived from AP and CD sample [48]. Cow dung derived porous carbon shows highest surface area value with micro and mesoporous nature due to nature of amorphous raw materials and preparation strategy adopted in the present method. The similar potential window is adopted for comparative super capacitance efficiency calculation in Table 5. Porous activated carbon derived from tire waste is activated by phosphoric acid method and it shows two-time lesser activity compared to present method. Hence, the clay molded calcination method is providing efficient surface area value, pore size distribution and active electrochemical property for super capacitor application.

In commercialization of modified electrode in Supercapacitors is to explore the long-term cycle duration and long-term cyclic stability for

Table 5
Comparative surface area and electrochemical activity of various precursor route prepared porous carbon materials.

Biomass precursors	Activating agent	S_{BET} (m^2/g)	C_{sp} (F/g)	Current density (A/g)	Electrolyte	Reference
Sugarcane bagasse	$ZnCl_2$	1788	300	0.25	1 M H_2SO_4	[39]
Rice husk	$ZnCl_2$	1442	243	0.05	6 M KOH	[41]
Human hair	KOH	1104	264	0.25	6 M KOH	[32]
Scrap waste tires	H_3PO_4	563	106	1	6 M KOH	[44]
Paulownia flower	KOH	1471	297	1	1 M H_2SO_4	[45]
Corn cob	HNO_3	543	221	0.5	0.5 M H_2SO_4	[48]
A. heterophyllus peel (AP)	H_3PO_4	1585	324	1	1 M Na_2SO_4	Present work
Cow dung (CD)	H_3PO_4	2450	347	1	1 M Na_2SO_4	Present work

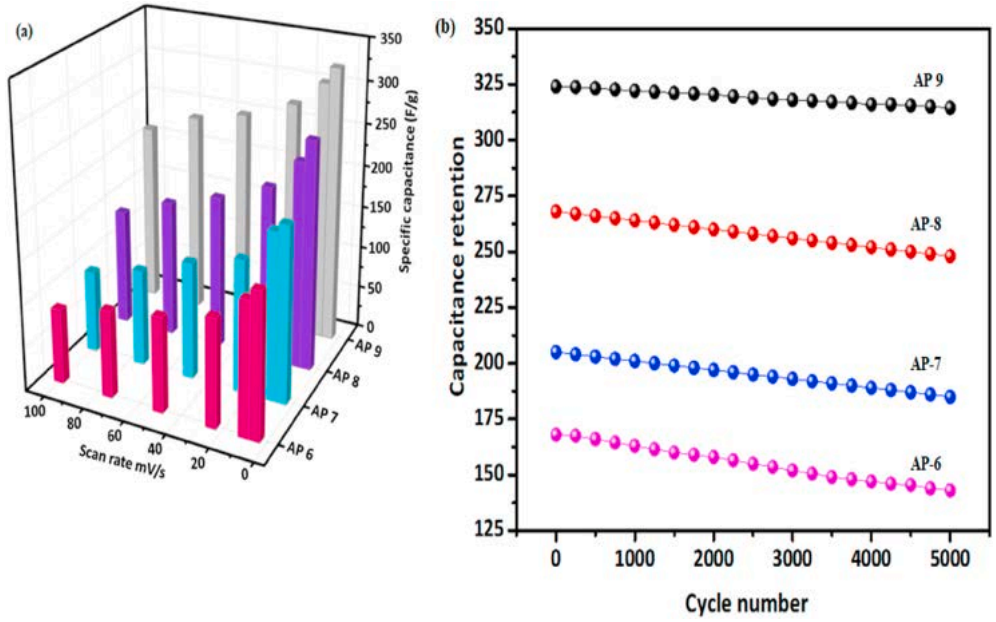

Fig. 13. (a) Specific capacitance Vs scan rate capacitance measurement for AP-6 to AP-9 (d) Cycle stability analysis for AP-6 to AP-9 samples.

the as-prepared porous activated carbon samples. Fig. 13 (a and b) shows the effect of scan rate for specific capacitance measurement for all peel waste derived carbon sample. At low scan rate the higher specific capacitance are obtained for AP-6 to AP-9 samples and the same trend was obtained in the case of CD-6 to CD-9. The cyclic stability of AP-6, AP- 7, AP-8 and AP- 9 samples tested at a current density of 1 A/g for 5000 cycles within a potential window from 0 to 0.68 V in 1 M Na_2SO_4 electrolyte using three electrode systems. From Fig. 13b shows the AP-9 sample indicates that there is no specific capacitance loss occurs after 5000 cycles and samples AP- 6, J AP-7 and AP- 8 show small loss in specific capacitance at the time of reaching 3500 cycles. The capacitance retention of AP-9 is 93%, which strongly demonstrates the excellent electrochemical stability of AP- 9 electrode material. The excellent electrochemical results of CD-9 and AP-9 was due to calcination treatment, high surface area and effective pore size distribution of the respective carbon samples.

5. Conclusion

Model solid bio-waste such as Jackfruit peel (AP) and Cow dung (CD) are successfully processed and developed as active carbon based modified electrodes. The phosphoric acid activation and clay molded calcination method was effective to produce high surface area carbon materials with multi porous architecture. The improved surface area values are useful for catalysis application and higher specific capacitance values are obtained for both AP-9 and CD-9 samples. The high specific capacitance with excellent long-term cyclic stability up to 5000 cycles has been achieved for both source derived carbon modified Nickle foil electrode. In future, as prepared carbon nanomaterial could be adopted to Nickel foil based flexible electrode device fabrication for renewable energy application.

Declaration of competing interests

The authors declare that they have no known competing financial interests or personal relationships that could have appeared to influence the work reported in this paper.

Acknowledgement

The authors are grateful to Deanship of Scientific research, King Saud University for financial support through vice Deanship of Research Chairs.

References

[1] L. Jiang, L. Sheng, Z. Fan, Biomass-derived carbon materials with structural diversities and their applications in energy storage, Sci. China Mater. 61 (2018) 133–158, https://doi.org/10.1007/s40843-017-9169-4.
[2] L. Li, N. Zhao, W. Wei, Y. Sun, A review of research progress on CO2 capture, storage, and utilization in Chinese Academy of Sciences, Fuel 108 (2013) 112–130, https://doi.org/10.1016/j.fuel.2011.08.022.
[3] V. Daioglou, A.P.C. Faaij, D. Saygin, M.K. Patel, B. Wicke, D.P. Van Vuuren, Energy demand and emissions of the non-energy sector, Energy Environ. Sci. 7 (2014) 482–498, https://doi.org/10.1039/c3ee42667j.
[4] C.L. Lee, P.S. H'Ng, M.T. Paridah, K.L. Chin, U. Rashid, M. Maminski, W.Z. Go, R. A. Raja Nazrin, S.N. Asyikin Rosli, P.S. Khoo, Production of bioadsorbent from phosphoric acid pretreated palm kernel shell and coconut shell by two-stage continuous physical activation via N2 and air, R. Soc. Open Sci. 5 (2018), https://doi.org/10.1098/rsos.180775.
[5] F.Z. Sobrosa, N.P. Stochero, E. Marangon, M.D. Tier, Development of refractory ceramics from residual silica derived from rice husk ash, Ceram. Int. 43 (2017) 7142–7146, https://doi.org/10.1016/j.ceramint.2017.02.147.
[6] B. Ramulu, G. Nagaraju, S.C. Sekhar, J.S. Yu, Waste tissue papers templated highly porous Mn3O4 hollow microtubes prepared via biomorphic method for pseudocapacitor applications, J. Alloys Compd. 772 (2019) 925–932, https://doi.org/10.1016/j.jallcom.2018.09.108.
[7] K.Y. Cheng, A.H. Kaksonen, G.B. Douglas, Bioresource Technology Sequential in situ hydrotalcite precipitation and biological denitrification for the treatment of high-nitrate industrial effluent, Bioresour. Technol. 172 (2014) 373–381, https://doi.org/10.1016/j.biortech.2014.09.050.
[8] E. Smidt, K.U. Eckhardt, P. Lechner, H.R. Schulten, P. Leinweber, Characterization of different decomposition stages of biowaste using FT-IR spectroscopy and pyrolysis-field ionization mass spectrometry, Biodegradation 16 (2005) 67–79, https://doi.org/10.1007/s10531-004-0430-8.
[9] S. Meng, Z. Mo, Z. Li, R. Guo, N. Liu, Effect of annealing temperature on the compositions and electrochemical performance of Mn_3O_4/γ-MnOOH composites on carbon cloth, Chem. Phys. Lett. 738 (2020), https://doi.org/10.1016/j.cplett.2019.136859.
[10] S.M. Majd, H. Teymourian, A. Salimi, Fabrication of an electrochemical l-cysteine sensor based on graphene nanosheets decorated manganese oxide nanocomposite modified glassy carbon electrode, Electroanalysis 25 (2013) 2201–2210, https://doi.org/10.1002/elan.201300245.
[11] V. Chaturvedi, S. Usangonvkar, M. V Shelke, Synthesis of high surface area porous carbon from anaerobic digestate and it's electrochemical study as an electrode material for ultracapacitors, RSC Adv. 9 (2019) 36343–36350, https://doi.org/10.1039/c9ra06603a.

[12] X. Yuan, M.-K. Cho, J.G. Lee, S.W. Choi, K.B. Lee, Upcycling of waste polyethylene terephthalate plastic bottles into porous carbon for CF4 adsorption, Environ. Pollut. 265 (2020), https://doi.org/10.1016/j.envpol.2020.114868.
[13] X. Yuan, S. Li, S. Jeon, S. Deng, L. Zhao, K.B. Lee, Valorization of waste polyethylene terephthalate plastic into N-doped microporous carbon for CO2 capture through a one-pot synthesis, J. Hazard Mater. 399 (2020), https://doi.org/10.1016/j.jhazmat.2020.123010.
[14] Y. Xie, J. Lin, H. Lin, Y. Jiang, J. Liang, H. Wang, S. Tu, J. Li, Removal of anionic hexavalent chromium and methyl orange pollutants by using imidazolium-based mesoporous poly(ionic liquid)s as efficient adsorbents in column, J. Hazard Mater. 392 (2020), https://doi.org/10.1016/j.jhazmat.2020.122496.
[15] T. Selkälä, T. Suopajärvi, J.A. Sirviö, T. Luukkonen, P. Kinnunen, K.I. Kling, J. B. Wagner, H. Liimatainen, Efficient entrapment and separation of anionic pollutants from aqueous solutions by sequential combination of cellulose nanofibrils and halloysite nanotubes, Chem. Eng. J. 374 (2019) 1013–1024, https://doi.org/10.1016/j.cej.2019.06.008.
[16] P. Karthikeyan, S. Vigneshwaran, J. Preethi, S. Meenakshi, Preparation of novel cobalt ferrite coated-porous carbon composite by simple chemical co-precipitation method and their mechanistic performance, Diam. Relat. Mater. 108 (2020), https://doi.org/10.1016/j.diamond.2020.107922.
[17] H. Wang, W. Zhang, P. Bai, L. Xu, Ultrasound-assisted transformation from waste biomass to efficient carbon-based metal-free pH-universal oxygen reduction reaction electrocatalysts, Ultrason. Sonochem. 65 (2020), https://doi.org/10.1016/j.ultsonch.2020.105048.
[18] F. Chen, Y. Ji, Y. Deng, F. Ren, S. Tan, Z. Wang, Ultrasonic-assisted fabrication of porous carbon materials derived from agricultural waste for solid-state supercapacitors, J. Mater. Sci. 55 (2020) 11512–11523, https://doi.org/10.1007/s10853-020-04751-y.
[19] R. Lahti, D. Bergna, H. Romar, T. Hu, A. Comazzi, C. Pirola, C.L. Bianchi, U. Lassi, Characterization of cobalt catalysts on biomass-derived carbon supports, Top. Catal. 60 (2017) 1415–1428, https://doi.org/10.1007/s11244-017-0823-z.
[20] M. Iwanow, T. Gärtner, V. Sieber, B. König, Activated carbon as catalyst support: precursors, preparation, modification and characterization, Beilstein J. Org. Chem. 16 (2020) 1188–1202, https://doi.org/10.3762/bjoc.16.104.
[21] I. Bordun, V. Pohrebennyk, O. Korostynska, V. Ptashnyk, M. Sadova, Agricultural waste as raw for electrode material of supercapacitors, in: Int. Multidiscip. Sci. GeoConference Surv. Geol. Min. Ecol. Manag. SGEM, 2016, pp. 365–370. https://www.scopus.com/inward/record.uri?eid=2-s2.0-85021680023&partnerID=40&md5=01c48f0d24f7dad03c1c4489dc883511.
[22] D.-W. Cho, J. Park, G. Kwon, J. Lee, G.-J. Yim, W. Jung, Y.-W. Cheong, Zirconia-Assisted pyrolysis of coffee waste in CO2 environment for the Simultaneous production of fuel gas and composite adsorbent, J. Hazard Mater. 386 (2020), https://doi.org/10.1016/j.jhazmat.2019.121989.
[23] P.R. Bonelli, A.L. Cukierman, Valorization of Wastes from Industrial Processing of an Agricultural Product via Thermochemical Conversion Processes, 2015. https://www.scopus.com/inward/record.uri?eid=2-s2.0-84956820226&partnerID=40&md5=d7384b11ca4e6eca6def41ad1aeb6af3.
[24] E. Santoso, R. Ediati, Y. Kusumawati, H. Bahruji, D.O. Sulistiono, D. Prasetyoko, Review on recent advances of carbon based adsorbent for methylene blue removal from waste water, Mater. Today Chem. 16 (2020), https://doi.org/10.1016/j.mtchem.2019.100233.
[25] S. Xia, N. Cai, J. Wu, H. Xiao, J. Hu, X. Chen, Y. Chen, H. Yang, X. Wang, H. Chen, Synthesis and formation mechanism of biomass-based mesoporous graphitic carbon, Fuel Process. Technol. 209 (2020), https://doi.org/10.1016/j.fuproc.2020.106543.
[26] M. Gao, W.-K. Wang, Y.-M. Zheng, Q.-B. Zhao, H.-Q. Yu, Hierarchically porous biochar for supercapacitor and electrochemical H2O2 production, Chem. Eng. J. 402 (2020), https://doi.org/10.1016/j.cej.2020.126171.
[27] G.A. Batista, M.L.M. Silva, W.P. Gomes, I.C.O. Neves, P.C.G. Mól, J. V de Resende, L.A.A. Veríssimo, J.R. Soares, Preparation of mesoporous activated carbon from defective coffee beans for adsorption of fresh whey proteins, Acta Sci. Technol. 42 (2020), https://doi.org/10.4025/actascitechnol.v42i1.45914.
[28] H. Chen, Z. Zhao, P. Qi, G. Wang, L. Shi, F. Yu, Sulphur-doped banana peel-derived activated carbon as electrode materials for supercapacitors, Int. J. Nanomanufacturing 15 (2019) 181–195, https://doi.org/10.1504/IJNM.2018.097253.
[29] P. Sennu, V. Aravindan, Y.-S. Lee, High energy asymmetric supercapacitor with 1D@2D structured NiCo2O4@Co3O4 and jackfruit derived high surface area porous carbon, J. Power Sources 306 (2016) 248–257, https://doi.org/10.1016/j.jpowsour.2015.12.029.
[30] J. Elisadiki, Y.A.C. Jande, R.L. Machunda, T.E. Kibona, Porous carbon derived from Artocarpus heterophyllus peels for capacitive deionization electrodes, Carbon N. Y. 147 (2019) 582–593, https://doi.org/10.1016/j.carbon.2019.03.036.
[31] S. Baskar, C. Murugesan, P. Barpanda, Highly porous n-doped graphitic carbon from bio-waste as bifunctional electrocatalyst for hybrid na-air battery, in: ECS Trans, 2017, pp. 425–430, https://doi.org/10.1149/08010.0425ecst.
[32] A. Sahasrabudhe, S. Kapri, S. Bhattacharyya, Graphitic porous carbon derived from human hair as 'green' counter electrode in quantum dot sensitized solar cells, Carbon N. Y 107 (2016) 395–404, https://doi.org/10.1016/j.carbon.2016.06.015.
[33] A. Miura, T. Kubota, K. Hamada, T. Hitomi, Adsorption efficiency of natural materials for lowconcentration cesium in solution, Water Sci. Technol. 73 (2016) 2453–2460, https://doi.org/10.2166/wst.2016.098.
[34] Y. Sun, I.K.M. Yu, D.C.W. Tsang, J. Fan, J.H. Clark, G. Luo, S. Zhang, E. Khan, N.J. D. Graham, Tailored design of graphitic biochar for high-efficiency and chemical-free microwave-assisted removal of refractory organic contaminants, Chem. Eng. J. 398 (2020), https://doi.org/10.1016/j.cej.2020.125505.
[35] P. Nshimiyimana, A. Messan, Z. Zhao, L. Courard, Chemico-microstructural changes in earthen building materials containing calcium carbide residue and rice husk ash, Construct. Build. Mater. 216 (2019) 622–631, https://doi.org/10.1016/j.conbuildmat.2019.05.037.
[36] A.B.D. Nandiyanto, Z.A. Putra, R. Andika, M.R. Bilad, T. Kurniawan, R. Zulhijah, I. Hamidah, Porous activated carbon particles from rice straw waste and their adsorption properties, J. Eng. Sci. Technol. 12 (2017) 1–11. https://www.scopus.com/inward/record.uri?eid=2-s2.0-85038859532&partnerID=40&md5=fa40a1c8322f8c8b95c871d7cf022b75.
[37] F. Mechati, C. Bouchelta, M.S. Medjram, R. Benrabaa, N. Ammouchi, Effect of hard and soft structure of different biomasses on the porosity development of activated carbon prepared under N2/microwave radiations, J. Environ. Chem. Eng. 3 (2015) 1928–1938, https://doi.org/10.1016/j.jece.2015.07.007.
[38] S. Roy, U. Kumar, P. Bhattacharyya, Synthesis and characterization of exfoliated biochar from four agricultural feedstock, Environ. Sci. Pollut. Res. 26 (2019) 7272–7276, https://doi.org/10.1007/s11356-018-04117-7.
[39] M. Imtiaz, Z. Chen, C. Zhu, H. Pan, I. Zada, Y. Li, S.W. Bokhari, R. Luan, S. Nigar, S. Zhu, In situ growth of β-FeOOH on hierarchically porous carbon as anodes for high-performance lithium-ion batteries, Electrochim. Acta 283 (2018) 401–409, https://doi.org/10.1016/j.electacta.2018.06.140.
[40] T. Adinaveen, L. John Kennedy, J. Judith Vijaya, G. Sekaran, Surface and porous characterization of activated carbon prepared from pyrolysis of biomass (rice straw) by two-stage procedure and its applications in supercapacitor electrodes, J. Mater. Cycles Waste Manag. 17 (2015) 736–747, https://doi.org/10.1007/s10163-014-0302-6.
[41] Y. Shen, Y. Zhou, Y. Fu, N. Zhang, Activated carbons synthesized from unaltered and pelletized biomass wastes for bio-tar adsorption in different phases, Renew. Energy 146 (2020) 1700–1709, https://doi.org/10.1016/j.renene.2019.07.167.
[42] H.C. Ho, M. Goswami, J. Chen, J.K. Keum, A.K. Naskar, Amending the structure of renewable carbon from biorefinery waste-Streams for energy storage applications, Sci. Rep. 8 (2018), https://doi.org/10.1038/s41598-018-25880-0.
[43] B. Yu, G. Jiang, C. Cao, N. Lei, C. Li, U. Evariste, P. Ma, Preparation and electrochemical properties of ultra-high specific surface area N-doped biomass-porous carbon, J. Energy Storage 30 (2020), https://doi.org/10.1016/j.est.2020.101537.
[44] K. Ding, L. Zhou, R. Qu, D. Zhang, J. Chen, X. He, L. Wang, H. Wang, H. Dou, Honeycomb-shaped carbon particles prepared from bicycle waste tires for anodes in lithium ion batteries, Mater. Chem. Phys. 251 (2020), https://doi.org/10.1016/j.matchemphys.2020.123202.
[45] J. Liu, L. Hao, W. Qian, Y.-F. He, R.-M. Wang, Mechanisms on formation of hierarchically porous carbon and its adsorption behaviors, Water Sci. Technol. 74 (2016) 266–275, https://doi.org/10.2166/wst.2016.195.
[46] W. Luo, B. Zheng, Improved electrochemical performance of LiNi 0.5 Co 0.2 Mn 0.3 O 2 cathode material by double-layer coating with graphene oxide and V 2 O 5 for lithium-ion batteries, Appl. Surf. Sci. 404 (2017) 310–317, https://doi.org/10.1016/j.apsusc.2017.01.200.
[47] Q. Yao, X. Zhou, S. Xiao, J. Chen, I.A. Abdelhafeez, Z. Yu, H. Chu, Y. Zhang, Amorphous nickel phosphide as a noble metal-free cathode for electrochemical dechlorination, Water Res. 165 (2019), https://doi.org/10.1016/j.watres.2019.114930.
[48] Y. Zhang, X. Song, P. Zhang, H. Gao, C. Ou, X. Kong, Production of activated carbons from four wastes via one-step activation and their applications in Pb2+ adsorption: insight of ash content, Chemosphere 245 (2020), https://doi.org/10.1016/j.chemosphere.2019.125587.